

Zr₄CuSb₇ – A PbFCl-related Polyantimonide, and Structure Relations of Zirconium-Transition Metal Polyantimonides

Magnus Greiwe and Tom Nilges

Fachgebiet Synthese und Charakterisierung innovativer Materialien, Department Chemie,
Technische Universität München, Lichtenbergstraße 4, 85747 Garching, Germany

Reprint requests to Prof. Dr. Tom Nilges. Fax: +49 89 289 13110. E-mail: tom.nilges@lrz.tum.de

Z. Naturforsch. **2014**, *69b*, 1124–1130 / DOI: 10.5560/ZNB.2014-4115

Received May 29, 2014

Dedicated to Professor Hubert Schmidbaur on the occasion of his 80th birthday

Single crystals of tetrazirconium copper heptaantimonide were obtained by arc-melting and annealing from the elements in ideal ratios including a 10% excess of Sb. The excess of Sb is needed to compensate for the evaporation loss during arc-melting synthesis. Zr₄CuSb₇ crystallizes tetragonally, space group *P4bm* (no. 100) as a racemic twin. It adopts a unique structure that can be regarded as a composite of a PbClF unit and a layered, partially copper-substituted polyantimonide substructure. Zr₄CuSb₇ represents a filling and substitution variant of the Hf₅Sb₉ structure type. The copper atoms fill voids and partially replace antimony atoms in the 4.8² Sb net of the Hf₅Sb₉ polyantimonide substructure to form a distorted 4⁴ net in Zr₄CuSb₇. Structure relations to known zirconium-transition metal polyantimonides are given, and new structures are predicted based on these relations.

Key words: Transition Metal Polyphosphide, Sb–Sb Bonding, Structure Chemistry of Polyantimonides

Introduction

Binary Zr/Hf polyantimonides and ternary Zr-transition metal polyantimonides have been subject to structure- and electrochemical investigations during the last 10 to 15 years. In 2004 Assoudet *al.* [1] reported on a new binary phase in the Hf-Sb system which is characterized by two building blocks, a PbFCl-related Hf-Sb substructure which is separated by a 4.8² net of Sb (for the PbFCl structure type see [2]). This structure was reported as $\sqrt{5} \times \sqrt{5}$ superstructure of the ZrSiS type [3] where a 4⁴ net of Si is separating the PbFCl block formed by Zr and S atoms [4]. This structure principle of an almost non-distorted PbFCl block, separated by a complex polyantimonide or antimonide net, is common and widespread for zirconium-transition metal polyantimonides. Examples are Zr₂T₂Sb₃ (with *T* = Cu, Pd) [5, 6] and Zr₃T₃Sb₇ (with *T* = Ni, Pd) [6, 7]. The separating unit in Zr₂T₂Sb₃ is a planar, non-corrugated 4⁴ net formed by *T* and Sb atoms while in Zr₃T₃Sb₇ the same 4⁴ net is only generated by Sb atoms. Recently, review articles on structure-chemical properties and the electrochemical performance of antimonides and polyan-

timonides have been published summarizing the intriguing structural chemistry and the performance of antimony-containing compounds as anodes for batteries [8, 9].

Results and Discussion

A crystal of the title compound suitable for single-crystal X-ray diffraction was separated directly from the annealed sample. The composition of the crystal was determined by energy dispersive X-ray spectroscopic analysis (EDS). Data were collected and averaged from three different points on the crystal surface resulting in 34(1) at-% Zr, 8(1) at-% Cu, and 58(1) at-% Sb. This composition is in good agreement with the composition derived from the structure refinement (see below). According to the empirical formula Zr₄CuSb₇, a composition of 33.3% Zr, 8.3% Cu and 58.3% Sb is expected.

Crystal structure of Zr₄CuSb₇

Zr₄CuSb₇ represents a derivative of the Hf₅Sb₉ structure type where the Zr and Sb atoms form

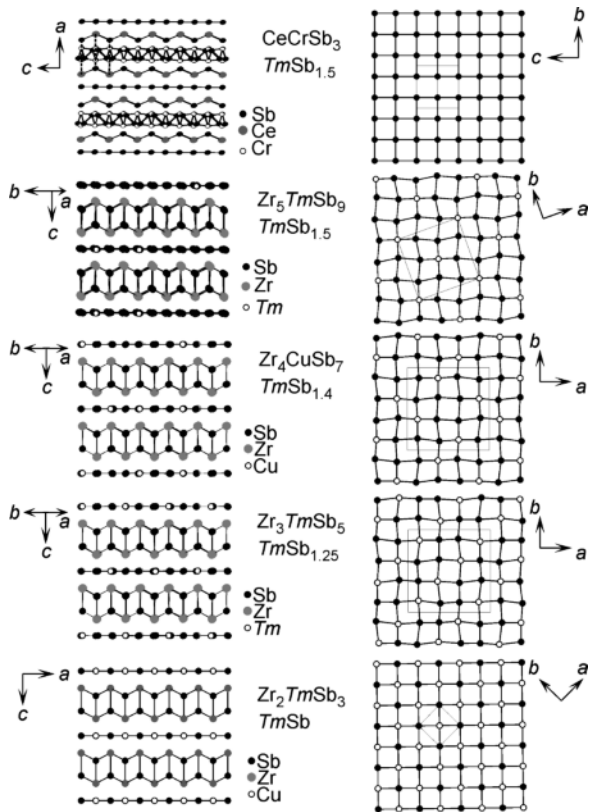


Fig. 1. Structure sections of transition metal polyantimonides TSb_{2-x} with $x = 0.5$ to 1. Examples are $TSb_{1.5}$ ($CeCrSb_3$ and Zr_5TmSb_9 of T_6Sb_9 type), $TSb_{1.4}$ (Zr_4CuSb_7), $TSb_{1.25}$ (Zr_3TmSb_5), and TSb (Zr_2TmSb_3) featuring PbFCl-related Zr/Sb blocks and T/Sb 4^4 nets with various compositions.

a PbFCl-related block, and the Cu and Sb atoms build up a distorted 4^4 net. The Sb substructure is related to the Sb substructure of Hf_5Sb_9 where a 4.8^2 net is present, separating a PbFCl unit. The Cu atoms located in close neighborhood to Sb in Zr_4CuSb_7 are filling a) all empty voids within the Hf_5Sb_9 -related 4.8^2 Sb net and b) partially replace Sb atoms within the 4.8^2 net to generate a distorted 4^4 net. A section of the structure of Zr_4CuSb_7 and the Sb substructure of Hf_5Sb_9 are given in Figs. 1 and 2, respectively. As a result of this partial Sb substitution, attractive Sb–Sb contacts of 2.976(1) and 2.990(1) Å remain within the distorted 4^4 net. Crystallographic data and atomic coordinates are summarized in Tables 1 and 2.

The Cu atoms are surrounded by Zr and Sb atoms with Cu–Sb distances of 2.587(1) to 2.622(1) Å and with Cu–Zr distances of 3.010(4) Å. In Zr_4CuSb_7 four

Table 1. Crystallographic data of Zr_4CuSb_7 .

Empirical formula	Zr_4CuSb_7
T , K	298(2)
M_r	1280.7
Crystal size, mm ³	$0.40 \times 0.27 \times 0.02$
Crystal system	tetragonal
Space group	$P4bm$
a , Å	11.1384(4)
c , Å	8.6813 (3)
V , Å ³	1077.04 (7)
Z	4
$D_{\text{calcd.}}$, g cm ⁻³	7.90
μ (MoK α), cm ⁻¹	23.2
$F(000)$, e	2184
hkl range	$\pm 15, -15$ to $+13, \pm 11$
$((\sin \theta)/\lambda)_{\text{max}}$, Å ⁻¹	0.694
Refl. measured/unique/ R_{int}	28 520/1246/0.098
Param. refined	68
$R(F)/wR(F^2)^a$ (all refl.)	0.0395/0.0922
Inversion twin ratio	0.53(5) : 0.47(5)
GoF (F^2)	1.31
$\Delta\rho_{\text{fin}}$ (max/min), e Å ⁻³	4.64/−3.89

different Zr positions are realized which are nine-fold coordinated by neighboring atoms. All coordination polyhedra of Zr to either $M = Sb$ or Cu are given in Fig. 3. The Zr– M distances between 2.925(3) and 3.160(2) Å are in good accordance with the respective Hf–Sb distances in Hf_5Sb_9 (2.8884(5) to 3.1792(5) Å).

All relevant distances are summarized in Table 3. Phase purity has been substantiated by powder X-ray diffraction. A representative powder diffractogram of Zr_4CuSb_7 is given in Fig. 4.

Structure relations of zirconium–transition metal polyantimonides and related compounds

At first glance $ZrSb_2$ [10, 11], Hf_5Sb_9 [1], Zr_4CuSb_7 , or Zr_2CuSb_3 [5] seem to have nothing in common but this is not true if one takes a detailed look on the structural features of each phase (Figs. 1 and 2). The structural chemistry of the title compound and related ternary zirconium-transition metal polyantimonides is dominated by a PbFCl-like substructure, separated by a complex antimony-containing network. A prototype of a zirconium compound with non-corrugated PbFCl-like building blocks separated by a planar 4^4 net is $ZrSiS$ [3]. Silicon is forming a regular 4^4 net, while the PbFCl units are constructed by Zr and S atoms (see Fig. 2). Based on these structural features the whole series of compounds TSb_{2-x} with

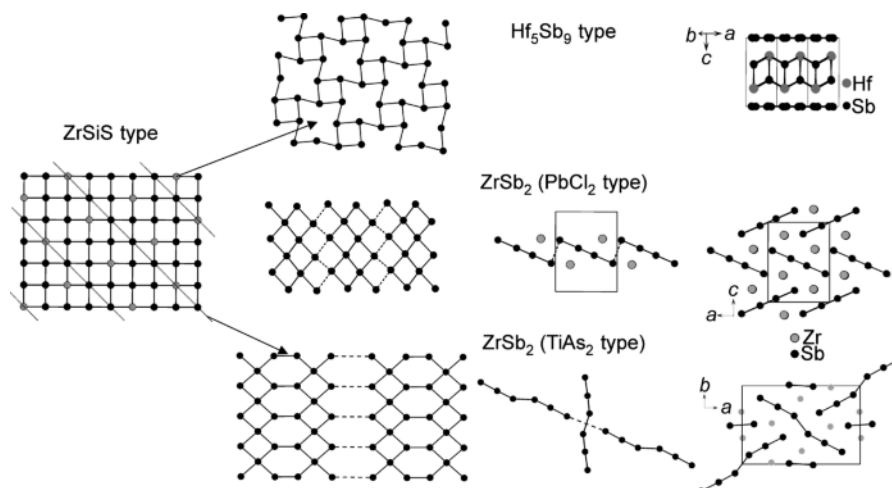


Fig. 2. Structure relations between the polyanionic substructures of Hf_5Sb_9 [1] or $ZrSb_2$ [10, 11] and regular 4^4 nets, realized e. g. in $ZrSiS$ [3]. Systematic generation of voids in a 4^4 net (left) by removal of grey atoms or atoms underneath the lines (left) leads directly to the polyanionide substructures of Hf_5Sb_9 or $ZrSb_2$ ($TiAs_2$ type [11]). The polyanionide substructure of $PbCl_2$ -type $ZrSb_2$ [10] can be derived from a 4^4 net by shearing fractions towards each other. A fully filled unit cell with completed polyantimonide substructure is given for each compound on the right hand side.

Atom	Wyckoff Site	x/a	y/b	z/c	U_{iso}
Sb1	2b	$\frac{1}{2}$	0	0.93403(15)	0.0046(4)
Sb2	2a	0	0	0.94763(19)	0.0036(3)
Sb3	4c	0.24692(6)	0.25308(6)	0.94293(17)	0.0033(3)
Sb4	4c	0.39123(5)	0.10877(5)	0.5578(2)	0.00605(16)
Sb5	8d	0.00282(6)	0.24923(4)	0.17470(12)	0.0052(3)
Sb6	8d	0.85823(5)	0.12484(5)	0.55606(14)	0.00594(14)
Zr1	2a	0	0	0.3010(2)	0.0024(4)
Zr2	4c	0.75362(8)	0.25361(8)	0.2931(2)	0.0031(4)
Zr3	2b	$\frac{1}{2}$	0	0.2848(3)	0.0040(5)
Zr4	8d	0.49535(9)	0.25114(6)	0.82117(15)	0.0036(4)
Cu1	4c	0.62598(10)	0.12598(10)	0.5512(6)	0.0102(4)

Table 2. Atomic coordinates and isotropic displacement parameters (\AA^2) for Zr_4CuSb_7 at 298 K.

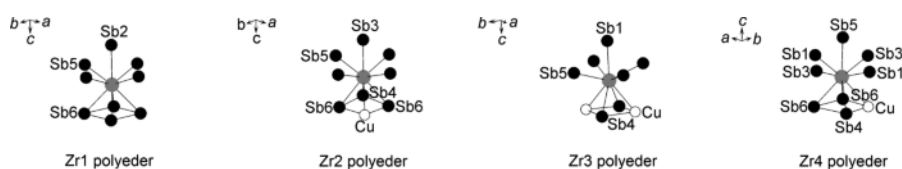


Fig. 3. Zr coordination polyhedra in Zr_4CuSb_7 .

$x = 0$ to 1 and T being one or two transition metals can be explained. In the following we discuss the structural similarities of the whole structure family (TSb_{2-x} with $x = 0$ to 1) in more detail, in order to systemize the structural chemistry and to unify or simplify the description of such complex structures. We also use this systematic approach to predict unknown phases. De-

tails of all realized and predicted compounds are given in Table 4.

Different approaches like void generation in the 4^4 net, substitution within the 4^4 net or a combination of both are needed to fully understand the formation of polyantimonide networks in such transition metal polyantimonides (TSb_{2-x} with $x = 0$ to 1).

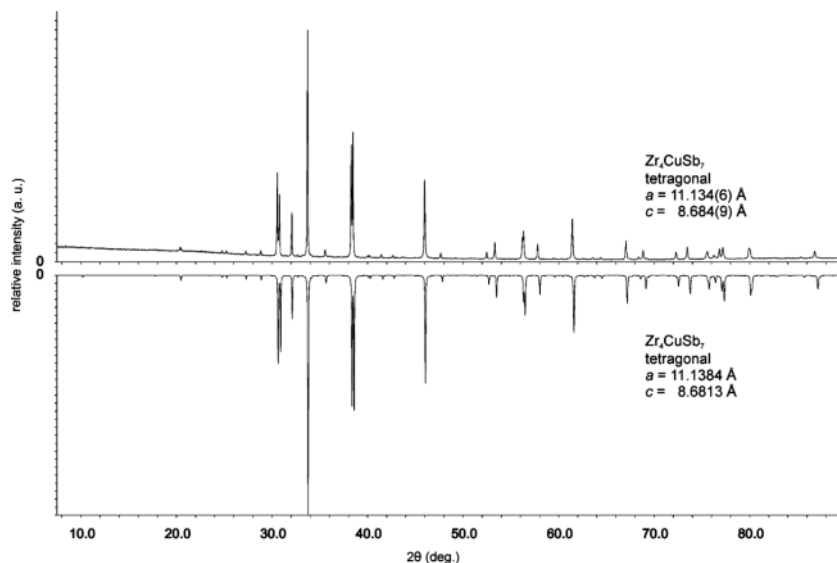


Fig. 4. Powder X-ray pattern of Zr₄CuSb₇. A calculated powder pattern derived from the single-crystal structure determination is drawn with negative intensities. No crystalline impurity was detected.

Table 3. Selected interatomic distances (< 3.1 Å) of Zr₄CuSb₇ at 298 K. Standard deviations are given in parentheses.

Sb1–Zr3	3.045(3)	Sb5–Zr1	2.985(1)
Sb1–Zr4 (2×)	2.9643(9)	Sb5–Zr2	2.960(1)
Sb1–Zr4 (2×)	2.9643(9)	Sb5–Zr2	2.977(1)
Sb2–Zr1	3.068(3)	Sb5–Zr3	2.9523(9)
Sb2–Zr4 (4×)	2.982(1)	Sb5–Zr4	3.070(1)
Sb3–Zr2	3.042(2)	Sb6–Zr1	3.054(2)
Sb3–Zr4 (2×)	2.962(1)	Sb6–Zr2	2.937(2)
Sb3–Zr4 (2×)	2.995(1)	Sb6–Zr4	3.088(2)
Sb4–Zr2	3.159(2)	Sb6–Zr4	2.967(2)
Sb4–Zr3	2.925(3)	Sb6–Cu1	2.587(1)
Sb4–Zr4 (2×)	3.014(2)	Zr2–Cu1	3.010(4)
Sb4–Cu1 (2×)	2.622(1)		

Starting with a regular 4⁴ net as shown in Figs. 1 and 2, voids can be generated in an ordered way to create the polyantimonide substructures of ZrSb₂ (TSb₂) or Hf₅Sb₉ (TSb_{1.8}). Dimorphic ZrSb₂ crystallizes in the PbCl₂ [10] and the TiAs₂ [11] structure types. In the PbCl₂-type ZrSb₂ a 4⁴ Sb net fragment is realized. This fragment can be directly derived from a 4⁴ net where the Zr atoms cut the entire 4⁴ net into smaller fragments which are then shorn towards each other. This process is illustrated in Fig. 2. The Sb substructure in TiAs₂-type ZrSb₂ seems to be more complex, and a 4⁴ Sb net fragment connected *via* a Sb–Sb dumbbell is present. The polyantimonide substructure can be

regarded as an arrangement of interpenetrating 4⁴ networks where two different sets of voids are generated in each of them. Such a removal of atoms from a 4⁴ net leads to the formation of six-membered rings neighbored to four-membered ones. One half of these voids is empty, and the other half is hosting the interpenetrating second 4⁴ net. A structure section is given in Fig. 2.

If the Sb content is reduced from TSb_{2.0} to TSb_{1.8}, the PbFCl-related block formed by T and Sb is separated by a 4.8² Sb net as represented by the binary polyantimonide Hf₅Sb₉. From a formal point of view the 4.8² net can be derived from a 4⁴ net by removing 20% of the atoms according Fig. 2.

Zr₃TSb₇ (with T = Ni, Pd) [6, 7] are representatives featuring a general composition of TSb_{1.75}. Two slightly corrugated building blocks, a 4⁴ Sb net and a PbFCl-related section formed by T, Zr and Sb atoms are present. These compounds are the only examples discussed herein where the replacement of transition metal atoms takes place in the PbFCl block (see Fig. 1). The Zr substitution within the PbFCl block obviously results in a slight corrugation of the two building blocks. From now on, the PbFCl block is the dominant structural feature in all further transition metal polyantimonides under discussion.

Table 4. Zirconium-transition metal polyantimonides TSb_{2-x} with $x = 0$ to 1 and structurally related compounds. The basic empirical formula, the T to Sb ratios of the different structure units, and predicted and realized compounds are denoted. Predicted compounds are written in *italics*, and the amount of voids within the structure units is given in roman numbers.

Basic formula	T : Sb atomic ratio in PbFCl block ^a	T : Sb ratio in Sb net, structure ^b	Compound realized	Compound predicted
TSb_2	n. a.	0 : 1, f	ZrSb ₂ (PbCl ₂ type)	
$TSb_{1.8}$	5 : 5	I : 3, interpen. c_o I : 4, defect p or 4.8^2 net	ZrSb ₂ (TiAs ₂ type) Hf ₅ Sb ₉	
$TSb_{1.75}$	n. a.	0 : 1, c_o and c_i	Zr ₃ NiSb ₇ Zr ₃ PdSb ₇	–
$TSb_{1.6}$	3 : 3	I : 5, c_o or c_i		<i>Zr₃TSb₈</i>
$TSb_{1.5}$	5 : 5	I : 4, p and c_i	Zr ₅ NiSb ₉	<i>Zr₅TSb₉</i>
$TSb_{1.5}$	1 : 1 (Ce : Sb) 1 : 1 (Cr : Sb) PbCl ₂ block	0 : 1, p_e	CeCrSb ₃	
$TSb_{1.4}$	4 : 4	I : 3, p and c_i	Zr ₄ CuSb ₇ (1)	
$TSb_{1.33}$	2 : 2	I : 2, p, c_i and c_o		<i>Zr₂TSb₄</i>
$TSb_{1.25}$	3 : 3	I : 2, p, c_i and c_o		<i>Zr₃TSb₅</i>
$TSb_{1.2}$	4 : 4	I : 2, p, c_i and c_o		<i>Zr₄TSb₆</i>
$TSb_{1.0}$	2 : 2	I : 1, p_e	Zr ₂ CuSb ₃ Zr ₂ PdSb ₃	

^a The atomic ratio is calculated for compounds featuring a PbFCl-like substructure and taking into account the side condition of a 1 : 1 ratio between the Sb network and the PbFCl block. Example calculation for Zr₄CuSb₇: a Sb net with T : Sb ratio = 1 : 3 results in a partial composition of CuSb₃. For the PbFCl block which itself always realizes a 1 : 1 T : Sb ratio, an atomic ratio of Zr₄CuSb₇-CuSb₃ = Zr₄Sb₄ or 4 : 4 results; ^b structure description codes: c_i = corrugated 4^4 network with different bond lengths within the network; c_o = corrugated 4^4 net with distortion of the whole net along the net plane; p = planar 4^4 net, non-corrugated in the direction of prolongation; p_e = planar 4^4 net, non-corrugated in the direction of prolongation, equidistant; f = fragmented 4^4 net.

A $TSb_{1.5}$ representative with a closely related structure is CeCrSb₃ [12]. Herein, an undistorted Sb 4^4 net is present. Beside this net, a PbFCl-related Ce/Sb substructure (1 : 1 Ce : Sb ratio) can be found where a Cr/Sb substructure with a Cr : Sb ratio of 1 : 2 is inserted. A structure section of CeCrSb₃ is given in Fig. 1 including the structural features of the Cr/Sb and Ce/Sb substructures. The Cr/Sb substructure shows similarities to the PbCl₂ structure.

Another possibility to build new structures is to fill voids in existing structures. Existing voids within the 4.8^2 Sb net in the Hf₅Sb₉ structure type might be fully filled by additional atoms, resulting in a compound with the general formula T_6Sb_9 (or $TSb_{1.5}$). The ratio of voids to atoms is 1 : 4. A possible structure model for such a filling variant is given in Fig. 1. We found strong evidences for the existence of Zr₅NiSb₉, following this suggested structure model.

The title compound Zr₄CuSb₇ represents a $TSb_{1.4}$ phase. Four Zr and Sb atoms per formula unit form the PbFCl block leaving one Cu and three Sb atoms per formula unit behind to form the separating network.

The Cu atoms fill voids and partially substitute Sb in a 4.8^2 net. This substitution pattern can also be derived from a common 4^4 net by an ordered substitution of Sb by Cu on neighboring atom positions. Each pair of substituted atoms is perpendicularly oriented towards each other as shown in Fig. 1. The atomic ratio of copper to antimony within the 4^4 net is 1 : 3.

Taking one of the interpenetrating Sb nets of the TiAs₂-type ZrSb₂ as a possible candidate to fill voids into account, we can predict another polyantimonide featuring a PbFCl block of Zr and Sb atoms, separated by a partially substituted polyantimonide 4^4 net. The voids of the six-membered rings (see the polyantimonide substructure of the TiAs₂-type ZrSb₂ in Fig. 2) can be fully filled leading to a compound of the $TSb_{1.4}$ type, but with a different substitution pattern within the 4^4 net. Here a linear arrangement of substituted atoms might be present where every third row of Sb atoms is replaced (see Fig. 1). The void to atom ratio is also 1 : 3 in the case of the TiAs₂-type ZrSb₂ nets, and we can therefore expect an overall composition of T_5Sb_7 . It is possible that a second polymorph

of Zr₄CuSb₇ might exist, or that the predicted phase can be realized with different transition metals like Pd or Ni beside Zr. Investigations in this direction are currently underway.

A further reduction of the antimony content between TSb_{1.4} and TSb in line with comparable structure-chemical features might be possible. If we stay with a non-substituted PbFCl block and reduce the *T* to Sb ratio within the 4⁴ net from 1 : 3 to 1 : 2, we end up with a substitution pattern where every second row of Sb atoms is substituted by *T*. A structure model is given in Fig. 1. Following the observed trend from the known compounds Zr₅TSb₉, Zr₄TSb₇ and Zr₂TSb₃ (or T₆Sb₉, T₅Sb₇ and T₃Sb₃, respectively), we expect a composition of Zr₃TSb₅ (T₄Sb₅ or TSb_{1.25}) for the missing compounds.

Known polyantimonides with antimony contents of TSb_{1.5} and below show a systematic ratio of *T* to Sb within the 4⁴ net from 1 : 4 (Zr₅NiSb₉), 1 : 3 (Zr₄CuSb₇) to 1 : 1 (Zr₂TSb₃). Only integer quantities of antimony are realized for this set of compounds. If we step away from integer numbers for the antimony content, a less systematic or disordered distribution of *T* in the compounds must be taken into account. Till now, we did not find any hints for a random distribution of the *T* (or Zr) atoms in our samples but such a possibility must be considered. According to our postulated formalism, phases like TSb_{1.33}, TSb_{1.2} or TSb_{1.1} might be accessible. For TSb_{1.33} a general formula of T₃Sb₄ can be predicted if the PbFCl block is formed by two Zr and two Sb atoms leaving one *T* and two Sb behind for the 4⁴ net, and Zr₂TSb₄ results as the target composition. In the case of TSb_{1.2} one can expect T₅Sb₆, leading to a composition of Zr₄TSb₆. In both predicted structures the *T* to Sb ratio of the 4⁴ net is 1 : 2.

Finally, when the antimony content is reduced to equimolar amounts (TSb), the resulting phases Zr₂TSb₃ (with *T* = Cu, Pd) [5, 6] are antimonides without any covalent Sb–Sb bonds. The PbFCl-like Zr/Sb substructure is neighbored by a 4⁴ net of alternating *T* and Sb atoms in a ratio of 1 : 1.

Experimental Section

Synthesis of Zr₄CuSb₇

1.1 g of Zr₄CuSb₇ was synthesized by arc-melting under dry high-purity argon on a water-cooled copper hearth. The

starting materials were used without further purification in form of shots for Zr (99.8 %, ABCR), shots for Cu (99.999 %, Chempur) and shots for Sb (99.999 %, Chempur). A ratio of Zr : Cu : Sb = 5 : 1 : 8.3 (in at-%) and a 10 wt-% excess of Sb was used for the synthesis. Approximately the same Sb weight loss was found during the melting process in the arc furnace. The sample was melted three times, after each melting step the regulus was turned around in order to yield a homogeneous sample. The metallic bulk regulus was finely ground, and the resulting powder was annealed at 1123 K for three days in evacuated quartz tubes.

Semi-quantitative EDS analysis of Zr₄CuSb₇

A crystal of the title compound suitable for single-crystal X-ray diffraction was separated directly from the annealed sample. The chemical composition of the crystal was determined by energy dispersive X-ray spectroscopy (EDS) using a SEM 5900LV (Jeol) scanning electron microscope. The acceleration voltage was 15 kV. The results averaged from three different randomly selected points of the crystal surface are in good agreement with the composition calculated from the structure refinement. We found a ratio (in at-%) of Cu : Zr : Sb = 8(1) : 34(1) : 58(1) Sb, in good accordance with the calculated ratio of 33.3 : 8.3 : 58.3.

X-Ray structure determination of Zr₄CuSb₇

A single crystal of Zr₄CuSb₇ suitable for structure determination was separated from the bulk residue. Intensity data were collected on a Stoe IPDS II diffractometer fitted with a Mo source (MoK_{α1}, λ = 0.71079 Å). Data were corrected for Lorentz and polarization effects prior to the cell refinement using the X-AREA program suite [13]. The crystal structure was solved by the Superflip routine [14], implemented in the program JANA2006 [15, 16], and was refined as a racemic twin using the non-centrosymmetric space group *P4bm*. A twin ratio of 0.53(5) : 0.47(5) was found. A centrosymmetric space group can be ruled out due to the orientation of the PbFCl blocks relative to each other within the unit cell.

Further details of the crystal structure investigation may be obtained from Fachinformationszentrum Karlsruhe, 76344 Eggenstein-Leopoldshafen, Germany (fax: +49-7247-808-666; e-mail: crysdata@fiz-karlsruhe.de, http://www.fiz-karlsruhe.de/request_for_deposited_data.html) on quoting the deposition number CSD-427673.

Acknowledgement

The authors acknowledge funding from the German Science Foundation (DFG) within the PAK 177 project and grant Ni1095/4–1.

- [1] A. Assoud, K. M. Kleinke, N. Soheilnia, H. Kleinke, *Angew. Chem. Int. Ed.* **2004**, *43*, 5260–5262.
- [2] W. Nieuwenkamp, J. M. Bijvoet, *Z. Kristallogr.* **1932**, *81*, 469–473.
- [3] H. Onken, K. Vierheilig, H. Hahn, *Z. Anorg. Allg. Chem.* **1964**, *333*, 267–279.
- [4] J. Xu, K. M. Kleinke, H. Kleinke, *Z. Anorg. Allg. Chem.* **2008**, *634*, 2367–2372.
- [5] N. Koblyuk, G. Melnyk, L. Romaka, O. I. Bodak, D. Fruchart, *J. Alloys Compd.* **2001**, 284–286.
- [6] M. Greiwe, M. Krause, O. Osters, A. Dorantes, M. Piana, T. Nilges, *Z. Naturforsch.* **2013**, *68b*, 979–986.
- [7] V. Romaka, A. Tkachuk, L. Romaka, *Acta Crystallogr.* **2008**, *E64*, i47.
- [8] M. Greiwe, T. Nilges, *Prog. Solid State Chem.* **2014**, doi:10.1016/j.prosolidstchem.2014.04.012.
- [9] F. Winter, R. Pöttgen, M. Greiwe, T. Nilges, *Rev. Inorg. Chem.* **2014**, doi: 10.1515/revic-2014-0003.
- [10] E. Garcia, J. D. Corbett, *J. Solid State Chem.* **1988**, *73*, 452–467.
- [11] D. Eberle, K. Schubert, *Z. Metallk.* **1968**, *59*, 306–308.
- [12] M. Brylak, W. Jeitschko, *Z. Naturforsch.* **1995**, *50b*, 899–904.
- [13] X-Area (version 1.52), Stoe & Cie GmbH, Darmstadt (Germany) **2011**.
- [14] L. Palatinus, G. Chapuis, *J. Appl. Crystallogr.* **2007**, *40*, 786–790.
- [15] V. Petříček, M. Dušek, L. Palatinus, JANA2006, The Crystallographic Computing System, Institute of Physics, Academy of Sciences of the Czech Republic, Prague (Czech Republic) **2006**.
- [16] V. Petříček, M. Dušek, L. Palatinus, *Z. Kristallogr.-Cryst. Mater.* **2014**, *229*, 345–352.